Bruch's Membrane Opening Minimum Rim Width Provides Objective Differentiation between Glaucoma and Nonglaucomatous Optic Neuropathies

JOHN C. LEANEY, VUONG NGUYEN, EDUARDO MIRANDA, YAEL BARNETT, KATE AHMAD, SUI WONG, AND MITCHELL LAWLOR

• PURPOSE: **A challenging clinical scenario is distinguishing between normal tension glaucoma (NTG) and non-glaucomatous optic neuropathies (NGON). The key to the assessment remains identifying the presence of optic nerve head cupping. Recent optical coherence tomography (OCT) measurements now allow objective assessment of cupping by minimum rim width at Bruch's membrane opening (MRW-BMO). This study assessed the hypothesis that the MRW-BMO measurement quantifies cupping and therefore can differentiate between NTG and NGON.**

• DESIGN: **Diagnostic evaluation with area under the curve.**

• METHODS: **Setting: multicenter tertiary hospitals and outpatient clinics. Patient population: 81 eyes of 81 patients were enrolled, 27 with NTG and 54 with NGON, including ischemic optic neuropathy, previous optic neuritis, and compressive and inherited optic neuropathies. All NGON patients with intraocular pressure >21 mm Hg, narrow drainage angles, or a family history of glaucoma were excluded. Observational procedure: optic disc OCT images were obtained of both the retinal nerve fiber layer thickness and the MRW-BMO. Main outcome measurements: the utility of the MRW-BMO in differentiating GON from NGON was assessed using the area under the curve (AUC) estimated from a logistic regression model.**

• RESULTS: **The 5-fold cross-validated AUC for glaucoma versus nonglaucoma from logistic regression models using MRW-BMO values from all sectors was 0.95 (95% confidence interval: 0.86-1.00).**

• CONCLUSIONS: **The measurement of MRW-BMO effectively differentiates between NTG and NGON with a high level of sensitivity and specificity. Incorporating this measurement into routine glaucoma assessment may provide a robust method of assisting clinicians to improve diagnosis and therefore treatment of optic nerve diseases.** **(Am J Ophthalmol 2020;218: 164–172. © 2020 Elsevier Inc. All rights reserved.)**

Accepted for publication May 25, 2020.

From the Faculty of Medicine (J.C.L., M.L.), Sydney University, Sydney, New South Wales, Australia; Sydney Eye Hospital (J.C.L., V.N., M.L.), Sydney, New South Wales, Australia; Neuro-ophthalmology Department (E.M., S.W.), Moorfields Eye Hospital, London, United Kingdom; Radiology Department (Y.B.), St. Vincent's Hospital, Sydney, New South Wales, Australia; and the Neurology Department (K.A.), North Shore Hospital, Sydney, New South Wales, Australia.

Inquiries to John C. Leaney, Sydney Eye Hospital, 8 Macquarie Street, Sydney, Australia 2000; e-mail: jcmleaney@gmail.com

OPTIC NERVE DYSFUNCTION OCCURS AMONG A heterogeneous group of diseases that may affect visual function. Glaucomatous optic neuropathy (GON) is the most common optic neuropathy worldwide,[1] but a range of nonglaucomatous optic neuropathies (NGON) also present with optic nerve head changes and visual field defects. These neuropathies include ischemic optic neuropathy, optic neuritis, compressive optic neuropathy, optic disc drusen, and inherited optic neuropathies.

Clinically differentiating between GON and NGON is critical as their natural histories, treatments, systemic associations, and propensity for visual impairment are different. A 15-year UK analysis found the highest payouts for medicolegal insurance claims related to missed or poorly followed intracranial tumors causing optic nerve head and visual field changes.[2]

The pathognomonic signs of GON are progressive loss of retinal ganglion cells with characteristic excavation of tissue at the optic nerve head, that is, optic disc cupping. There have been case reports of cupping in NGON, but those cases are the exception rather than the rule.[3] Although the assessment of optic nerve head cupping may be more straightforward in advanced disease, for many cases, the cup size assessment is challenging in part because the there is an arbitrary reference plane distinguishing the rim from the cup.[4]

This distinction has been tested empirically, and expert clinical assessment of the optic nerve head alone was found to be inaccurate in diagnosing different types of optic nerve pathologies.[5] A number of clinicians in the study diagnosed glaucoma in patients with nonglaucomatous diseases. The relatively poor performance of expert assessment is likely to be exacerbated by more widespread adoption of optical coherence tomography (OCT) by other health professionals including optometrists.

0002-9394/$36.00
https://doi.org/10.1016/j.ajo.2020.05.034

TABLE 1. Mean Ratios for and Visual Fields for GON and NGON[a]

	GON	NGON	*P* Value
Number of Eyes	27	54	
Mean ± SD MD visual field	−7.7 ± 7.2	−11.6 ± 8.6	.054
Mean ± SD MRW-BMO			
PO1-ST	180.3 ± 84.7	264.6 ± 102.3	.004
PO2-IT	145.4 ± 61.2	318.3 ± 107.3	<.001
PO3-Temporal	155.4 ± 52.9	214.1 ± 78.8	.004
SO1-Global	196.9 ± 55.5	291.9 ± 85.0	<.001
SO2-Nasal	239.0 ± 69.9	319.5 ± 96.2	.003
SO3-SN	229.8 ± 71.2	315.0 ± 99.8	.003
SO4-IN	210.1 ± 76.0	366.3 ± 106.8	<.001
Mean ± SD ratio (MRW-BMO/RNFLT)			
PO1-ST	2.1 ± 0.9	3.8 ± 1.8	.002
PO2-IT	2.1 ± 1.3	3.6 ± 1.8	.004
PO3-Temporal	2.9 ± 1	4.7 ± 2.1	.002
SO1-Global	2.8 ± 0.6	4.8 ± 1.6	<.001
SO2-Nasal	3.5 ± 0.8	7.1 ± 3.6	.001
SO3-SN	2.6 ± 0.7	5.6 ± 2.8	.001
SO4-IN	2.8 ± 1.3	5.4 ± 2.3	<.001

BMO = Bruch's membrane opening; GON = glaucomatous optic neuropathy; IN = inferonasal; IT = inferotemporal; MD = mean deviation; MRW = minimum rim width; NGON = nonglaucomatous optic neuropathy; PO = primary outcome; RNFLT = retinal nerve fiber layer thickness; SD = standard deviation; SN = superonasal; SO = secondary outcome; ST = superotemporal

[a]*P* values were obtained from univariate logistic regression models assessing whether variables were significantly associated with the presence of glaucoma and adjusted for multiple comparisons using the Holm-Bonferroni correction.

A number of different clinical tests have been suggested for differentiating between GON and NGON.[6–12] Although elevated intraocular pressure (IOP) is a risk factor for GON, it is not useful for differentiating between GON and NGON. Population-based studies confirm that GON with "normal" IOP is common. In a US population, 50% of new diagnoses of GON had an IOP <22 mm Hg,[13] whereas the figure for a Japanese population was 92%.[14] Conversely, having a common disease such as glaucoma does not protect against dual pathology such as an intercurrent pituitary tumor. Color vision has also been suggested to be useful in differentiating GON from NGON, but the empirical evidence in support of this assertion is limited.[9] There is therefore a need to develop an objective measurement to assist in differentiating GON from NGON in patients with optic nerve disease.

The availability of OCT has introduced a new level of quantitative assessment of optic nerve disease.[15–17] Thinning of the peripapillary retinal nerve fiber layer (RNFL) occurs regardless of the underlying optic neuropathy and so does not distinguish between GON and NGON. However, the recent description of the measurement of the minimum rim width at Bruch's membrane opening (MRW-BMO) now provides an objective quantitative measurement of cupping.[18] One study has reported that MRW-BMO is able to distinguish between GON and nonarteritic anterior ischemic optic neuropathy,[19] but it has not been established whether this is the case with a more heterogenous group of patients with NGON.

We hypothesized that in a cohort of patients with established optic nerve disease and RNFL thinning, NGON patients will have relatively normal MRW-BMO measurements (no cupping), whereas GON will have abnormal MRW-BMO, ie both cupping and peripapillary RNFL loss. Recruitment was limited to patients with normal-tension glaucoma (NTG) rather than high-tension glaucoma as this is the group of patients most frequently investigated for causes of NGON.[9]

A tightly phenotyped group of patients with NTG was examined and compared to patients with a range of NGON to assess whether the MRW-BMO was effective in differentiating the two groups.

SUBJECTS AND METHODS

• **PATIENTS:** Subjects were enrolled consecutively into a diagnostic evaluation study using area under the curve analysis (AUC) recruited from 2 centers, one in Sydney, Australia, and the other in London, United Kingdom. The protocol and study design in Australia were approved prospectively by the South Eastern Sydney Area Health Network Human Research Ethics Committee (reference

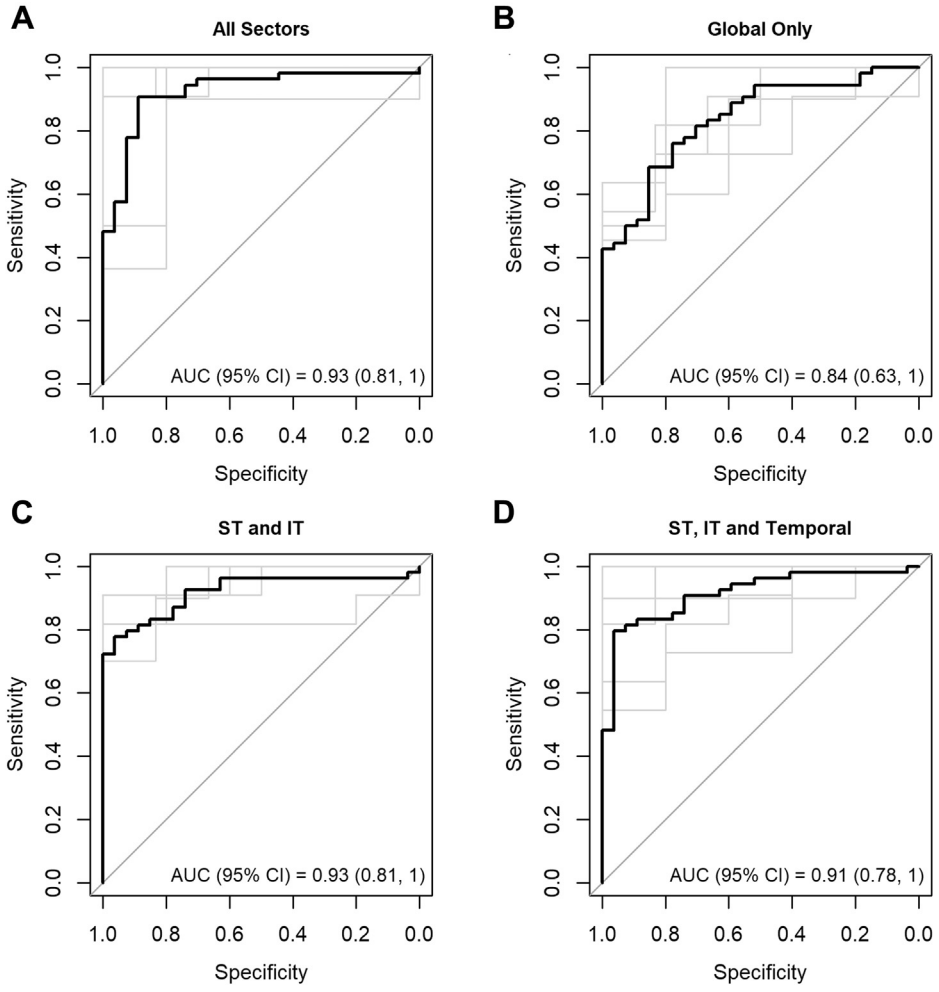

FIGURE 1. Receiver operator characteristic and area under the curve (AUC) from 5-fold cross-validated logistic models using MRW-BMO from (A) all sectors, (B) global measurement only, (C) superotemporal (ST), and inferotemporal (IT) sectors; and (D) ST, IT, and temporal sectors. Curves for individual folds are shown in light gray. MRW-BMO = minimum rim width at Bruch's membrane opening.

number 16/055). In the United Kingdom, the study was registered retrospectively as an audit of practice (institutional review board reference CA18/NO/01). Informed consent was obtained from all patients. All testing was conducted according to the tenets of the Declaration of Helsinki.

• **INCLUSION AND EXCLUSION CRITERIA:** NTG patients had their diagnoses confirmed by a fellowship-trained glaucoma subspecialist based on characteristic optic disc appearance with matching glaucomatous visual field loss. IOP had never to have been recorded above 21 mm Hg, and all patients had open drainage angles with dark room gonioscopy. Secondary glaucomas such as pseudoexfoliation and pigment dispersion syndrome were excluded.

Other exclusion criteria included age younger than 18 years, significant media opacity, clinical evidence of diabetic retinopathy, and macular degeneration or any other retinal disease. Any participants unable or unwilling to undergo magnetic resonance imaging (MRI) of the brain and orbits with contrast were excluded.

NGON was diagnosed by a fellowship-trained neuro-ophthalmologist. Non-arteritic anterior ischemic optic neuropathy required documented painless disc swelling with visual field defects that either improved or stabilized over a 6-week period.[20] A "disc at risk" was required in the contralateral eye and, if the patient was older than 50 years of age, an erythrocyte sedimentation rate and a C-reactive protein assay with normal results were also required. Arteritic anterior ischemic optic neuropathy or posterior ischemic optic neuropathy required a positive temporal artery biopsy. Prior optic neuritis was diagnosed based upon a clinical history consistent with optic neuritis and a contrast-enhanced MRI demonstrating optic nerve enhancement at the time the patient was symptomatic. Patient conditions were diagnosed with drusen on the basis of the International Drusen Collaboration

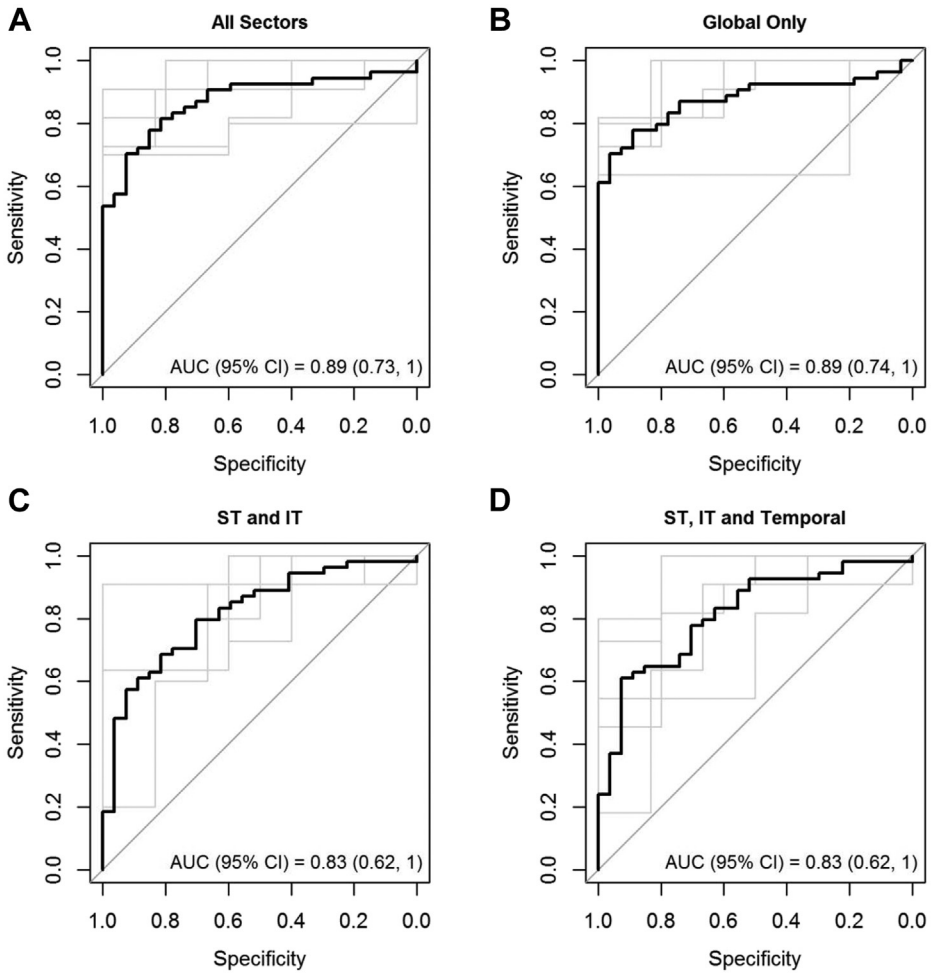

FIGURE 2. Receiver operator characteristic and area under the curve (AUC) from 5-fold cross-validated logistic models using MRW-BMO to RNFLT ratios from (A) all sectors, (B) global measurement only, (C) superotemporal (ST), and inferotemporal (IT) sectors; and (D) ST, IT, and temporal sectors. Curves for individual folds are shown in light gray. MRW-BMO = minimum rim width at Bruch's membrane opening.

recommendations.[21] All hereditary optic neuropathies were included only if genetic testing confirmed a known mutation for the condition. Any NGON patient with IOP >21 mm Hg, narrow drainage angles, or a known family history of glaucoma were excluded.

All subjects underwent a complete ophthalmic examination including best-corrected visual acuity, near vision, color vision (Ishihara plates), IOP with Goldmann applanation tonometry, Humphrey visual field ([Humphrey Field Anaylser 2 [HFA2], Carl Zeiss Meditec, Dublin, CA] 24-2; SITA-standard, white on white), optical coherence tomography (OCT) (Spectralis OCT [Heidelberg Engineering, Heidelberg, Germany] MRW-BMO, retinal nerve fibre layer [RNFL] thickness [RNFLT], ganglion cell complex), and optic nerve head photos [Zeiss Visucam, Carl Zeiss Meditec, Jena, Germany]).

All NTG patients underwent blood tests for full blood count, electrolytes, urea, creatinine, vitamin B_{12}, and folate and an MRI of the brain and orbits with gadolinium enhancement using a standard protocol.

The OCT was performed by a trained technician at each facility. Only OCT scans with a mean quality score >15 were included for analysis. The scanning protocols for the Spectralis OCT followed previously published protocols.[18] Briefly, the MRW-BMO scanning pattern is a radial scan consisting of 24 equally distributed high-resolution 15-degree B-scans which compute the neuroretinal rim measurements. B-scans were averaged from 20 to 30 individual B-scans, with 768 A-scans per B-scan, centered on the optic nerve head. The RNFLT is a circumpapillary 12-degree circular scan with 1,536 A-scans centered on the optical nerve head. The data is averaged from 16 individual B-scans.

The MRW-BMO scan has a global value which is segmented into 6 sectors (temporal, nasal, superotemporal [ST], inferotemporal [IT], superonasal [SN], and

TABLE 2. Performance Metrics for Models Tested Using Different Combinations of MRW-BMO-to-RNFLT Ratios[a]

MRW-BMO						
Model	Sensitivity (95% CI)	Specificity (95% CI)	PPV (95% CI)	NPV (95% CI)	LRP (95% CI)	LRN (95% CI)
All sectors	0.89 (0.71-0.98)	0.93 (0.82-0.98)	0.86 (0.67-0.96)	0.94 (0.84-0.99)	5.71 (2.76-11.81)	0.30 (0.16-0.57)
Global only	0.63 (0.42-0.81)	0.83 (0.71-0.92)	0.65 (0.44-0.83)	0.82 (0.69-0.91)	3.60 (1.94-6.69)	0.41 (0.24-0.71)
ST and IT sectors	0.74 (0.54-0.89)	0.91 (0.80-0.97)	0.80 (0.59-0.93)	0.88 (0.76-0.95)	5.43 (2.51-11.30)	0.34 (0.19-0.61)
ST, IT and Temporal sectors	0.81 (0.62-0.94)	0.91 (0.80-0.97)	0.81 (0.62-0.94)	0.91 (0.80-0.97)	5.43 (2.51-11.30)	0.34 (0.19-0.61)
Post-hoc comparison[b]						
GON vs. ION	0.74 (0.54-0.89)	0.73 (0.50-0.89)	0.77 (0.56-0.91)	0.70 (0.47-0.87)	2.71 (1.32-5.57)	0.36 (0.18-0.71)
GON vs. non-ION	0.85 (0.66-0.96)	0.84 (0.67-0.95)	0.82 (0.63-0.94)	0.87 (0.70-0.96)	5.45 (2.40-12.38)	0.18 (0.07-0.44)
MRW-BMO ratios						
Model	Sensitivity (95% CI)	Specificity (95% CI)	PPV (95% CI)	NPV (95% CI)	LRP (95% CI)	LRN (95% CI)
All sectors	0.78 (0.58-0.91)	0.85 (0.73-0.93)	0.72 (0.53-0.87)	0.88 (0.77-0.96)	5.25 (2.68-10.27)	0.26 (0.13-0.53)
Global only	0.67 (0.46-0.83)	0.85 (0.73-0.93)	0.69 (0.48-0.86)	0.84 (0.71-0.92)	4.50 (2.25-9.00)	0.39 (0.23-0.67)
ST and IT sectors	0.63 (0.42-0.81)	0.83 (0.71-0.92)	0.65 (0.44-0.83)	0.82 (0.69-0.91)	3.78 (1.95-7.33)	0.44 (0.27-0.74)
ST, IT and Temporal sectors	0.67 (0.46-0.83)	0.87 (0.75-0.95)	0.72 (0.51-0.88)	0.84 (0.72-0.92)	5.14 (2.45-10.79)	0.38 (0.22-0.66)
Post-hoc comparison[b]						
GON vs. ION	0.89 (0.71-0.98)	0.81 (0.60-0.95)	0.86 (0.67-0.96)	0.86 (0.64-0.97)	4.89 (2.00-11.98)	0.14 (0.04-0.40)
GON vs. non-ION	0.81 (0.62-0.94)	0.75 (0.57-0.88)	0.73 (0.54-0.88)	0.83 (0.64-0.94)	3.25 (1.74-6.10)	0.25 (0.11-0.56)

CI = confidence interval; GON = glaucoma optic neuropathy; ION = ischemic optic neuropathy; IT = inferotemporal; LRP = likelihood ratio positive; LRN = likelihood ratio negative; PPV = positive predictive value; NPV = negative predictive value; ST = superotemporal.

[a]Post hoc models compared GON to ION and GON to all non-ION.

[b]Models for post-hoc comparisons used all sectors.

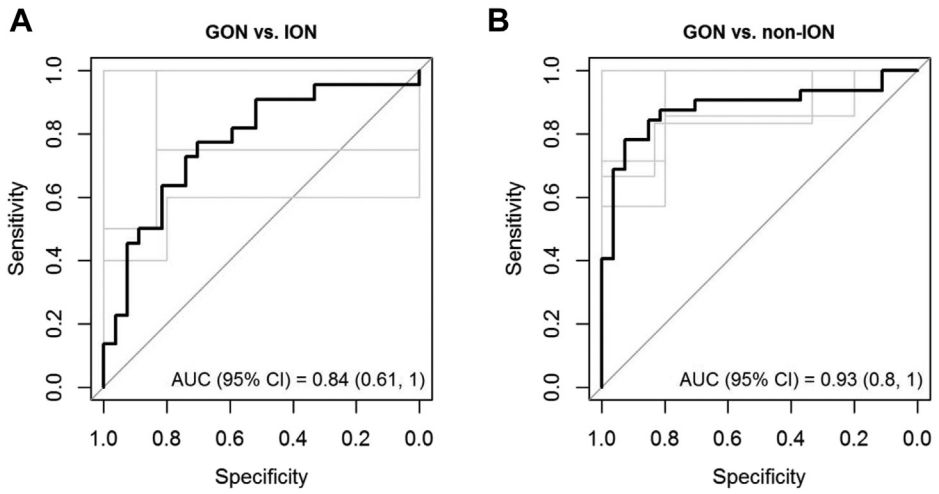

FIGURE 3. Receiver operator characteristic and area under the curve (AUC) from 5-fold cross-validated logistic models using minimum rim width at Bruch's membrane opening comparing (A) glaucomatous optic neuropathy (GON) to ischemic optic neuropathy (ION) and (B) GON to all non-ION. Models used minimum rim width at Bruch's membrane opening to RNFLT ratios from all sectors. Curves for individual folds are shown in light gray. RNFLT = retinal nerve fiber layer thickness.

inferonasal [IN]). The BMO was identified automatically by the software but was manually checked by a single operator and corrected in case of any segmentation or BMO location errors.

Only 1 eye for each patient was included in the study. If both eyes were eligible, the worst affected eye was included for analysis.

• **STATISTICAL ANALYSIS:** Univariate logistic regression models were used to assess whether the MRW-BMO measurement was significantly associated with the presence of GON. This was analysis was followed by 5-fold cross-validated logistic regression to assess the model's predictive power to classify GON versus NGON. AUC, sensitivity, specificity, positive predictive values (PPV), negative predictive values (NPV), and likelihood ratios were calculated from the cross-validated model. The positive likelihood ratio (PLR) was calculated as sensitivity/(1-specificity), and the negative likelihood ratio (NLR) was calculated as the (1-sensitivity)/specificity. A higher PLR (>1) gives an increased probability of having a disease following a positive test result, whereas a lower NLR (between 0 and 1) gives a lower probability of having a disease following a negative test result. For reference, a PLR of 5 represents an approximate increase of 30% in the post-test probability of having a disease, whereas an NLR of 0.2 represents an approximate decrease of 30% in the post-test probability of a patient having a disease. Four pre-specified models were analyzed using different combinations of MRW-BMO measurements: 1) all 6 sectors; 2) of only the global measurement; 3) of only the ST and IT sectors; and 4) of only the ST, IT, and temporal sectors. For each of the sectors, both the MRW-BMO alone, to distinguish GON from NGON, and the MRW-BMO-to-RNFL ratio were analyzed. The rationale for the latter was that it would anatomically match the sector of cupping with any associated RNFL loss in that particular sector.

All analyses were conducted using R version 3.5.1 software (R Project, Vienna, Austria) with the caret application (version 6.0-80) for cross-validation of logistic regression models and the pROC application (version 1.13.0) for plotting receiver operating characteristic (ROC) curves.

RESULTS

81 PATIENTS WERE RECRUITED. THIS INCLUDED 27 PATIENTS with NTG and 54 patients with a range of other optic neuropathies including ischemic (22), previous optic neuritis (14), compressive (8), disc drusen (4), inherited (3), toxic/nutritional (2) and traumatic (1). All NTG patients had a normal MRI brain and orbits with gadolinium, as assessed by a specialist neuro-radiologist. Baseline blood tests for the NTG subjects were within normal limits.

Mean MRW-BMO measurements and mean ratios of MRW-BMO:RNFL of the primary (ST, IT, temporal sectors) and secondary outcome measures (global, nasal, SN, IN) are shown in Table 1. Both the MRW-BMO and ratio measurements in the GON group were significantly lower than the NGON group. Visual field MD was more negative in the NGON group compared with the GON group (-11.6 vs. -7.7; $P = .054$).

ROC curves from cross-validated logistic regression are shown in Figures 1 and 2. Sensitivities, specificities, PPVs, NPVs, PLRs and NLRs are reported in Table 2. The models using all the sectors had the highest mean

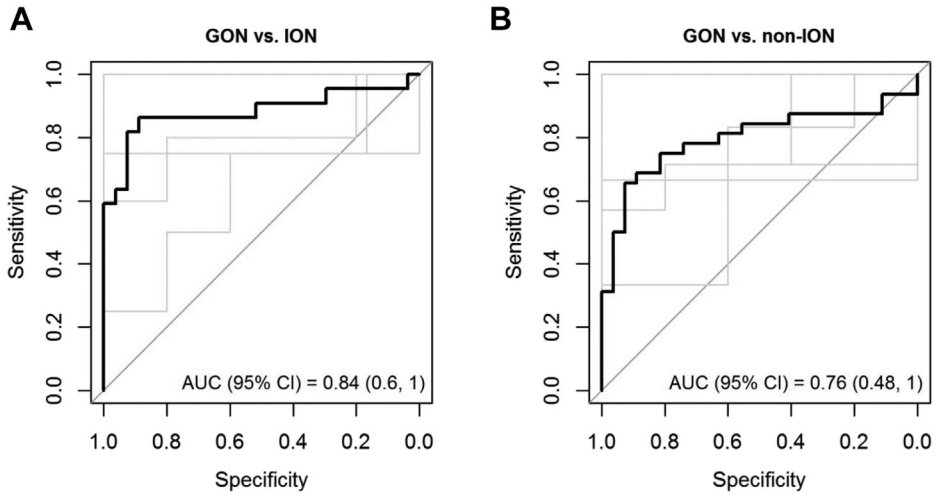

FIGURE 4. Receiver operator characteristic and area under the curve (AUC) from 5-fold cross-validated logistic models using minimum rim width at Bruch's membrane opening to RNFLT ratios comparing (A) glaucomatous optic neuropathy (GON) to ischemic optic neuropathy (ION) and (B) GON to all non-ION. Models used minimum rim width at Bruch's membrane opening to RNFLT ratios from all sectors. Curves for individual folds are shown in light gray. RNFLT = retinal nerve fiber layer thickness.

AUC when using the MRW-BMO values (AUC = 0.95 [95% confidence interval [CI]: 0.86-1]) or the MRW-BMO ratios (AUC = 0.89 [95% CI: 0.73-1]). The model using all sectors also had the highest PLR (5.71 [95% CI: 2.76-11.81] and 5.25 [95% CI: 2.68-10.27] using the MRW-BMO and ratios, respectively) and lowest NLR (0.30 [95% CI: 0.16-0.57] and 0.26 [95% CI: 0.13-0.53] using the MRW-BMO and ratios, respectively).

When GON was compared with ischemic optic neuropathy (ION) only (Figures 3 and 4), the AUC was 0.84 (95% CI: 0.61-1) and 0.84 (95% CI: 0.6-1) when using the MRW-BMO values and ratios, respectively. Likewise, when GON patients were compared to non-ION patients, the AUC was 0.93 (95% CI: 0.8-1) and 0.76 (95% CI: 0.48-1) when using the MRW-BMO values and ratios, respectively.

DISCUSSION

IN A CLINIC-BASED POPULATION OF TIGHTLY PHENOTYPED NTG and NGON patients, the MRW-BMO provides good objective differentiation between the 2 groups.

Optic nerve head cupping is the hallmark of glaucoma and relates to retinal ganglion cell death and the complex interplay of biomechanical factors specific to glaucoma, including ischemia, physical compression of axonal bodies, and tissue remodeling.[22] Glaucomatous cupping is often referred to as laminar or deep cupping to distinguish it from other types of nonglaucomatous cupping.[23] There is some suggestion that glaucomatous cupping has a greater anterior laminar depth than nonglaucomatous cupping.[24] Nonglaucomatous cupping appears to be confined to a subset of NGON which includes arteritic ischemic optic neuropathy,[25] dominant optic atrophy,[26] and some compressive optic neuropathies.[27,28]

For each of the present study's predefined outcome measurements, the device global measurement provided the highest level of sensitivity and specificity for differentiating GON from NGON. Although the sensitivity and specificity values of these models were good, clinicians and their patients are more interested in a slightly different question: given a positive (or negative) test result, what is the probability that the patient actually has NGON (or GON)? These values are represented by PPV and NPV. PPV and NPV values are influenced by the prevalence of the disease of interest. Higher disease prevalence will lead to more false negatives, whereas a lower disease prevalence will lead to more false positives. Likelihood ratios can be useful alternatives to provide post-test probabilities of having a disease following a positive or negative test based on the pretest probability. The low prevalence of NGON within clinical practice means this algorithm is more likely to generate false positives while reducing false negatives. For vision- and life-threatening diseases, the focus is on minimizing false negatives, accepting that the cost of this may be increased false positives.

Although the ratio of MRW-BMO:RNFL is unlikely to be sufficient to make a clinical differentiation alone, one current clinical limitation to detecting NGON is that clinicians may not consider it. GON is much more common, and cognitive biases may mean that an abnormal disc and visual field are more readily considered signs of glaucoma, without considering other possibilities. In high-resource environments, OCT is becoming routine in the assessment of glaucoma patients, and this creates the situation where the MRW-BMO may be included in routine clinical

practice through the OCT platform. The clinician would be alerted to the possibility of NGON and then be prompted to perform further targeted examinations to decide whether other investigations are required. This may mean checking color vision, reassessing the visual fields to consider whether they respect the vertical, or re-examining the disc to consider whether it is actually pale rather than cupped. In addition to alerting the clinician about alternative possible diagnoses, the MRW-BMO result could also assist in diagnosis by applying the result as part of a Bayesian approach, taking into account other clinical factors shown to differentiate between GON and NGON, such as anterior lamellar depth.[24]

Although these results assist in differentiating GON from NGON, they do not provide any assistance in subtyping which specific NGON may be presented. Further larger data sets for less common NGON may help to identify characteristic OCT findings that assist in differentiating each of these conditions. This is likely to be of most use in inherited optic neuropathies and compressive optic neuropathies that can be clinically the most challenging to differentiate from glaucoma. The present study was underpowered to comment on whether the MRW-BMO-to-RNFL ratio was different between different types of NGON such as arteritic versus nonarteritic anterior ischemic optic neuropathy, but mapping objective measurements of these phenotypes would be clinically useful.

The present study limitation is that it is a consecutive clinic-based study. Although the patient diagnoses reflect the relative incidence of optic neuropathies encountered in clinical practice, it is not guaranteed that these findings will extrapolate to each individual subtype of NGON.

ALL AUTHORS HAVE COMPLETED AND SUBMITTED THE ICMJE FORM FOR DISCLOSURE OF POTENTIAL CONFLICTS OF INTEREST and none were reported.

Funding/Support: Sydney Hospital Foundation, Sydney Eye Hospital, 8 Macquarie St, Sydney Australia, 2000. The sponsor had no role in the design or conduct of this research.

Financial Disclosures: The authors have reported that they have no relationships relevant to the contents of this paper to disclose.

REFERENCES

1. Tham YC, Li X, Wong TY, Quigley HA, Aung T, Cheng CY. Global prevalence of glaucoma and projections of glaucoma burden through 2040: a systematic review and meta-analysis. *Ophthalmology* 2014;121:2081–2090.
2. Mathew RG, Ferguson V, Hingorani M. Clinical negligence in ophthalmology: fifteen years of national health service litigation authority data. *Ophthalmology* 2013;120:859–864.
3. Piette SD, Sergott RC. Pathological optic-disc cupping. *Curr Opin Ophthalmol* 2006;17:1–6.
4. Reis AS, O'Leary N, Yang H, et al. Influence of clinically invisible, but optical coherence tomography detected, optic disc margin anatomy on neuroretinal rim evaluation. *Invest Ophthalmol Vis Sci* 2012;53:1852–1860.
5. O'Neill EC, Danesh-Meyer HV, Kong GX, et al. Optic disc evaluation in optic neuropathies: the optic disc assessment project. *Ophthalmology* 2011;118:964–970.
6. Danesh-Meyer HV, Boland MV, Savino PJ, et al. Optic disc morphology in open-angle glaucoma compared with anterior ischemic optic neuropathies. *Invest Ophthalmol Vis Sci* 2010; 51:2003–2010.
7. Boland MV, McCoy AN, Quigley HA, et al. Evaluation of an algorithm for detecting visual field defects due to chiasmal and postchiasmal lesions: the neurological hemifield test. *Invest Ophthalmol Vis Sci* 2011;52:7959–7965.
8. Rosdahl JA, Asrani S. Glaucoma masqueraders: diagnosis by spectral domain optical coherence tomography. *Saudi J Ophthalmol* 2012;26:433–440.
9. Fraser CL, White AJR, Plant GT, Martin KR. Optic nerve cupping and the neuro–ophthalmologist. *J Neuroophthalmol* 2013;33:377–389.
10. Danesh-Meyer HVMDF, Yap JM, Frampton CBHP, Savino PJMD. Differentiation of compressive from glaucomatous optic neuropathy with spectral-domain optical coherence tomography. *Ophthalmology* 2014;121:1516–1523.
11. Lee EJ, Yang HK, Kim T-W, Hwang J-M, Kim Y-H, Kim C-Y. Comparison of the pattern of retinal ganglion cell damage between patients with compressive and glaucomatous optic neuropathies. *Invest Ophthalmol Vis Sci* 2015;56:7012–7020.
12. Nakano E, Hata M, Oishi A, et al. Quantitative comparison of disc rim color in optic nerve atrophy of compressive optic neuropathy and glaucomatous optic neuropathy. *Graefes Arch Clin Exp Ophthalmol* 2016;254:1609–1616.
13. Sommer A, Tielsch JM, Katz J, et al. Relationship between intraocular pressure and primary open angle glaucoma among white and black Americans. The Baltimore Eye Survey. *Arch Ophthalmol* 1991;109:1090–1095.
14. Iwase A, Suzuki Y, Araie M, et al. The prevalence of primary open-angle glaucoma in Japanese: the Tajimi study. *Ophthalmology* 2004;111:1641–1648.
15. Schuman JS, Hee MR, Arya AV, et al. Optical coherence tomography: a new tool for glaucoma diagnosis. *Curr Opin Ophthalmol* 1995;6:89–95.
16. Schuman JS. Spectral domain optical coherence tomography for glaucoma (an AOS thesis). *Trans Am Ophthalmol Soc* 2008;106:426–458.
17. Barboni P, Savini G, Parisi V, et al. Retinal nerve fiber layer thickness in dominant optic atrophy measurements by optical coherence tomography and correlation with age. *Ophthalmology* 2011;118:2076–2080.
18. Chauhan BC, O'Leary N, Almobarak FA, et al. Enhanced detection of open-angle glaucoma with an anatomically accurate optical coherence tomography-derived neuroretinal rim parameter. *Ophthalmology* 2013;120:535–543.
19. Resch H, Mitsch C, Pereira I, et al. Optic nerve head morphology in primary open-angle glaucoma and nonarteritic anterior ischaemic optic neuropathy measured with

spectral domain optical coherence tomography. *Acta Ophthalmol* 2018;96:e1018–e1024.
20. Hayreh SS. Ischemic optic neuropathy. *Prog Retin Eye Res* 2009;28:34–62.
21. Malmqvist L, Bursztyn L, Costello F, et al. The Optic Disc Drusen Studies Consortium recommendations for diagnosis of optic disc drusen using optical coherence tomography. *J Neuroophthalmol* 2018;38:299–307.
22. Burgoyne CF. A biomechanical paradigm for axonal insult within the optic nerve head in aging and glaucoma. *Exp Eye Res* 2011;93:120–132.
23. Burgoyne CF, Downs JC. Premise and prediction-how optic nerve head biomechanics underlies the susceptibility and clinical behavior of the aged optic nerve head. *J Glaucoma* 2008;17:318–328.
24. Fard MA, Moghimi S, Sahraian A, Ritch R. Optic nerve head cupping in glaucomatous and non-glaucomatous optic neuropathy. *Br J Ophthalmol* 2019;103:374–378.
25. Danesh-Meyer HV, Savino PJ, Sergott RC. The prevalence of cupping in end-stage arteritic and nonarteritic anterior ischemic optic neuropathy. *Ophthalmology* 2001;108:593–598.
26. Fournier AV, Damji KF, Epstein DL, Pollock SC. Disc excavation in dominant optic atrophy: differentiation from normal tension glaucoma. *Ophthalmology* 2001;108:1595–1602.
27. Qu Y, Wang YX, Xu L, et al. Glaucoma-like optic neuropathy in patients with intracranial tumours. *Acta Ophthalmol* 2011;89:e428–e433.
28. Manor RS. Documented optic disc cupping in compressive optic neuropathy. *Ophthalmology* 1995;102:1577–1578.